Journal of
Medicinal Chemistry

Article

Discovery of (2R)-N-[3-[2-[(3-methoxy-1-methyl-pyrazol-4-yl)amino]pyrimidin-4-yl]-1H-indol-7-yl]-2-(4-methylpiperazin-1-yl)propenamide (AZD4205) as a potent and selective Janus Kinase 1 (JAK1) inhibitor

Qibin Su, Erica Banks, Geraldine Bebernitz, Kirsten Bell, Cassandra F. Borenstein, Huawei Chen, Claudio Chuaqui, Nanhua Deng, Andrew D. Ferguson, Sameer P. Kawatkar, Neil P. Grimster, Linette Ruston, Paul Lyne, Jon A. Read, Xian You Peng, Xiaohui Pei, Stephen Fawell, Zhanlei Tang, Scott Throner, Melissa Marie Vasbinder, Haoyu Wang, Jon Winter-Holt, Richard Woessner, Allan Wu, Wenzhan Yang, Michael Zinda, and Jason Grant Kettle

J. Med. Chem., **Just Accepted Manuscript** • DOI: 10.1021/acs.jmedchem.9b01392 • Publication Date (Web): 16 Apr 2020

Just Accepted

is published by the American Chemical Society. 1155 Sixteenth Street N.W., Washington, DC 20036

Discovery of (*2R*)-N-[3-[2-[(3-methoxy-1-methyl-pyrazol-4-yl)amino]pyrimidin-4-yl]-*1H*-indol-7-yl]-2-(4-methylpiperazin-1-yl)propenamide (AZD4205) as a potent and selective Janus Kinase 1 (JAK1) inhibitor

Qibin Su*,[1] Erica Banks,[1] Geraldine Bebernitz,[1] Kirsten Bell,[1] Cassandra F. Borenstein,[1] Huawei Chen,[1] Claudio E. Chuaqui,[1] Nanhua Deng,[1] Andrew D. Ferguson,[2] Sameer Kawatkar,[1] Neil P. Grimster,[1] Linette Ruston,[1] Paul D. Lyne,[1] Jon A. Read,[3] Xianyou Peng,[4] Xiaohui Pei,[4] Stephen Fawell,[1] Zhanlei Tang,[4] Scott Throner,[1] Melissa M. Vasbinder,[1] Haoyu Wang, [4] Jon Winter-Holt,[5] Richard Woessner,[1] Allan Wu,[2] Wenzhan Yang,[6] Michael Zinda,[1] Jason G. Kettle[5]

[1]Oncology R&D, AstraZeneca R&D, Waltham, MA 02451 USA. [2]Discovery Sciences, R&D, AstraZeneca R&D, Waltham, 02451 MA USA. [3]Discovery Sciences, R&D, AstraZeneca R&D, Cambridge, UK. [4] Pharmaron Beijing Co., Ltd., 6 Taihe Road, BDA, Beijing, 100176. [5]Oncology R&D, AstraZeneca R&D, Cambridge, UK. [6]Early Product Development, Pharmaceutical Sciences, R&D, 02451 Boston, USA.

Abstract: JAK1 together with JAK2, JAK3, and TYK2 belong to the JAK (Janus kinase) family. They play critical roles in cytokine signaling. Constitutive activation of JAK/STAT pathways are associated with a wide variety of diseases. Particularly, pSTAT3 is observed in response to the treatment with inhibitors of oncogenic signaling pathways such as EGFR, MAPK and AKT, and is associated with resistance or poorer response to agents targeting these pathways. Amongst the JAK family kinases, JAK1 has been shown to be the primary driver of STAT3 phosphorylation and signaling, therefore selective JAK1 inhibition can be a viable means to overcome such treatment resistances. Herein,

an account of the medicinal chemistry optimization from a promiscuous kinase screening hit **3** to the candidate drug **21** (AZD4205), a highly selective JAK1 kinase inhibitor, is reported. Compound **21** has good preclinical pharmacokinetics. Compound **21** displayed an enhanced antitumor activity in combination with approved EGFR inhibitor, osimertinib, in a preclinical non-small cell lung cancer (NSCLC) xenograft NCI-H1975 model.

Introduction

JAK1 together with JAK2, JAK3, and TYK2 belong to the JAK (Janus-associated kinase) family of cytoplasmic tyrosine kinases that play important roles in cytokine and growth factor mediated signal transduction.[1] Consequently, the JAK family kinases are strongly associated with both cancer[2] and inflammatory[3] diseases. Currently, there are several approved JAK inhibitors to treat human diseases: *tofacitinib* (Xeljanz®, a pan-JAK inhibitor from Pfizer)[4] for rheumatoid arthritis, *ruxolitinib* (**1**, Jakafi®, a selective JAK1/2 inhibitor from Incyte)[5] for intermediate- or high-risk myeloproliferative neoplasms and baricitinib (Olumiant®, a JAK1/2 inhibitor)[6-7] for the treatment of rheumatoid arthritis, together with peficitinib (Smyraf®, a pan-JAK inhibitor)[8-9] approved in Japan for treatment of RA. Both compounds have demonstrated clinical benefit in a range of disease areas, but have additionally been associated with a number of side effects. Specifically, tofacitinib's adverse events have included non-serious infections, reduction of leukocyte cell count number, and rare but severe incidences of perforation of the stomach or intestine. With ruxolitinib treatment, thrombocytopenia and anemia were observed.[10] These toxicities are believed to be associated with inhibition of JAK2. Thus, the pharmaceutical industry has been motivated to evaluate second generation inhibitors, which possess increased JAK isoform selectivity in the hope that treatment with such agents may maintain similar efficacy to established therapies, but with fewer undesirable side effects. To this end, JAK1

selective inhibitors (e.g. ABT494[11], PF-04965842[12], and filgotinib[13]) are currently being studied in human clinical trials for the treatment of autoimmune or inflammatory diseases.[14-15]

We have a long-standing interest in studying JAK inhibition in the area of oncology.[16-22] There is growing evidence to suggest that disregulation of constitutively activated JAK/STAT signaling is associated with a wide variety of malignancies.[23] In particular, increased activation of STAT3 through phosphorylation at Y705 (pSTAT3) is reported in up to 70% of human tumors including ovarian, breast, liver, prostate, colorectal, head and neck, esophageal, pancreatic, bladder, and non-small-cell lung cancers.[24-31] In addition, such elevated pSTAT3 has also been observed in response to chemotherapy treatment, and is associated with resistance or poor response to the treatment with agents targeting oncogenic signaling pathways such as EGFR, MAPK and AKT.[32-34] Amongst the JAK family kinases, JAK1 has been shown to be the primary driver of STAT3 phosphorylation and signaling.[35] JAK2, however, is essential for signal transduction downstream of erythropoietin, thrombopoietin and other related receptors that control erythrocyte and megakaryocyte expansion.[36] Taken together, it is believed that a JAK1 selective inhibitor may enable higher target coverage of the JAK1-STAT3 signaling by sparing toxicities such as thrombocytopenia and anemia, associated with JAK2 inhibition, thereby, maximizing the clinical benefit of such agents in oncology[10] and other therapeutic areas[37]. Herein, an account of the medicinal chemistry optimization from a promiscuous kinase screening hit **3** to the candidate drug **21** (AZD4205), a highly selective JAK1 kinase inhibitor, is reported. Detailed biological and pharmacokinetic evaluation of this compound is also included.

Results and Discussion

During the course of our discovery program, a patent application describing JAK1 selective inhibitors, such as compound **2**, were reported.[38] We synthesized and tested this compound in house. To our surprise, although derived from the same chemical class as **1**, a dual JAK1/2 inhibitor (JAK1 IC_{50} = 0.02 μM, no selectivity of JAK1 over JAK2), compound **2** displayed a high degree of JAK1 selectivity (JAK1 IC_{50} = 0.02 μM, 120-fold selectivity of JAK1 over JAK2). In order to rationalize the observed selectivity, an X-ray crystal structure of **2** bound to the kinase domain of JAK1 was solved (Figure 1, Panel A).

Table 1. Biochemical potencies of **1**, JAK1 selective inhibitor **2** and in-house screening hit **3**

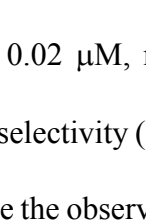

1

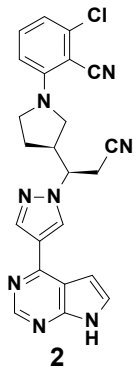

2

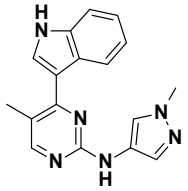

3

Compound	JAK1 IC_{50} (μM) [a]	JAK2 IC_{50} (μM) [a]	Selectivity over JAK2 (fold) [b]
1	0.02	0.02	1
2	0.02	2.4	120
3	0.07	0.38	5

[a]Biochemical potency was measured at 5 mM ATP concentration. [b]Selectivity expressed as the ratio of JAK2 IC_{50} over JAK1 IC_{50}. All experimental values represent the geometric mean of at least two independent experiments and have SEM within 0.2 log units. For experimental details, see the supporting information of reference.[22]

Analysis of the X-ray structure revealed a bidentate interaction between pyrrolopyrimidine moiety of **2** with hinge residues Glu957 and Leu959. The pyrrolopyrimidine and the pyrazole ring form hydrophobic interactions with Leu881, Val889 and Leu1010. The

nitrile group occupies a small pocket, formed by the isobutyl sidechain of Leu101 and Gly1020 and may stabilize the conformation of the pyrrolidine ring while possibly contributing to desolvation of this hydrophobic region. However, most interestingly, a well-ordered p-loop region with clear electron density is seen in the crystal structure. In general, the p-loop in kinases is very flexible. And it is common to observe poor or no electron density visible for this region even in high-resolution protein kinase structures.[39] The presence of such a well-ordered p-loop region suggests a stabilizing interaction between the terminal chloro-cyano-phenyl group of **2** and the hydrophobic pocket defined by the sidechains of protein residues Gly884, His885, Phe886 and Gly1028 of JAK1. We hypothesized that this stabilization is contributing to the JAK1 selectivity of **2**, because, in this region, there is a productive π- π stacking interaction between the chloro-cyano-phenyl group of **2** and the imidazole side chain of His885 in JAK1, which is absent in JAK2, where the corresponding residue is an asparagine.

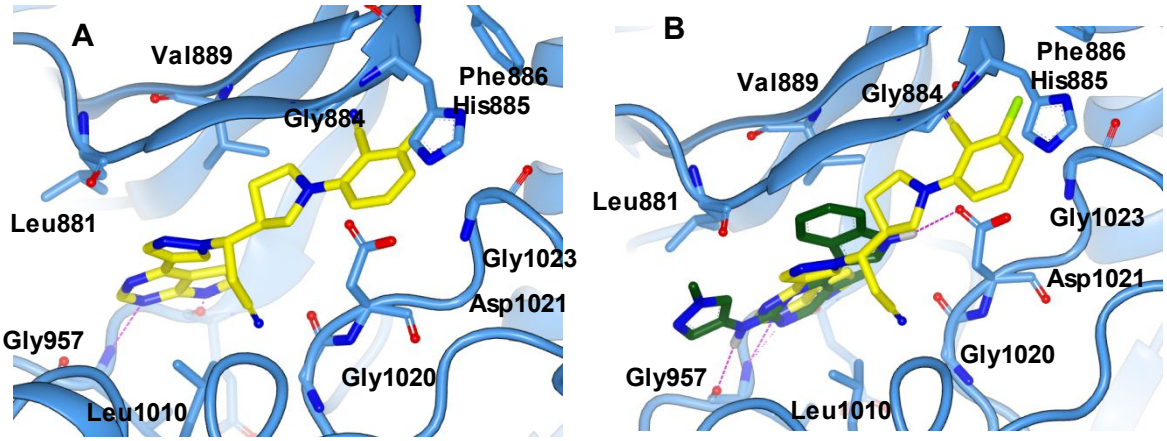

Figure 1. (A) X-ray crystal structure of **2** (yellow carbon atoms) bound to JAK1 (PDB code: 6SM8) reveals a p-loop JAK1 selectivity pocket. Selected residues are shown as sticks. Hydrogen bonds are shown as dotted lines. (B) Overlay of **3** (green carbon atoms) with x-ray

crystal structure of JAK1 in complex with compound **2** suggested substitutions of 7-position of indole ring can reach the p-loop selectivity pocket.

Our program started with a high through-put screen of the AstraZeneca compound collection against JAK1 to generate three-point IC_{50}s values. The resulting hits were followed-up in a five-point IC_{50} dose response versus JAK1 and JAK2, at the corresponding Km ATP concentrations (55 and 15 μM, respectively), in order to identify potent and selective starting points. In the lead optimization phase, we increased the ATP concentration to a more physiologically relevant level in our biochemical assays (5 mM) to assess the inhibitors' JAK1 potency and their selectivity towards JAK2. Herein, all the biochemical potencies are reported under the 5 mM ATP conditions.

From the screening campaign, compound **3** was identified as a potent JAK1 inhibitor (Table 1, IC_{50} = 0.07 μM) with moderate selectivity over JAK2 (JAK2 IC_{50} = 0.38 μM, 5-fold selectivity). Docking of **3** into the JAK1 protein showed that the indole NH binds the carboxylate moiety of Asp1021, while the 2-amino pyrimidine forms interactions with the hinge residue Leu959. Intriguingly, when superimposing[40] the docked pose of **3** onto the X-ray structure of **2**, we postulated that the 7-position of the indole may direct substituents toward the p-loop, thereby accessing the JAK1 selectivity pocket (Figure 1, Panel B). Consequently, we designed 7-substituted indole analogs containing an appropriate linker to direct an aryl group to the selectivity pocket and achieve the desired π-π interaction with His885, in the hopes of increasing the isoform selectivity of newly generated compounds. To test this hypothesis, with a consideration of ease of synthesis, **4**, bearing an amido-linker, was synthesized and evaluated in the JAK1 and JAK2 biochemical assays. As shown in Table 2, **4** displayed an increased JAK1

potency (IC_{50} = 0.004 μM), and more importantly with improved selectivity (50-fold) toward JAK2, compared to **3** (5-fold).

Table 2. SAR of JAK1 selective 4-pyrimidine indoles with varied linkers and solvent tails

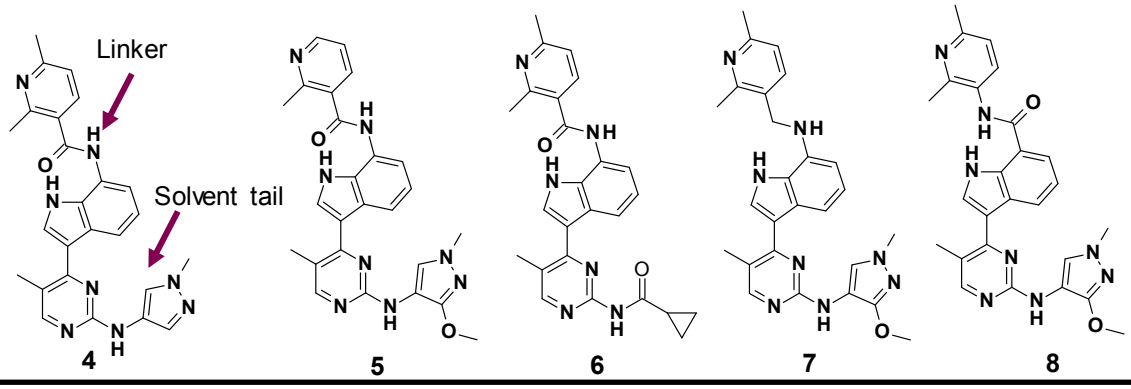

4 **5** **6** **7** **8**

Compound	JAK1 IC_{50} (μM) [a]	JAK2 IC_{50} (μM) [a]	Selectivity over JAK2 (fold)	Solubility (μM)[b]
4	0.004	0.20	50	--
5	0.018	2.2	122	41
6	0.043	2.5	58	2
7	0.004	0.56	140	0.1
8	0.26	> 30	115	0.1

[a] Biochemical potency was measured at 5 mM ATP concentration. Selectivity expressed as the ratio of JAK2 IC_{50} over JAK1 IC_{50}. All experimental values represent the geometric mean of at least two independent experiments and have SEM within 0.2 log units. For experimental details, see the supporting information.[22] [b]Solubility was measured at pH = 7.4.

With this encouraging result, we then turned our attention to explore the SAR of solvent tail groups (denoted as in **4**, Table 2). It has been reported that *ortho*-substitution on similar solvent tails may reduce JAK2 activity, thus improving selectivity between JAK1 and JAK2.[22] Capitalizing on this observation, we designed and synthesized **5** with a 3-methoxy-1-methyl amino-pyrazole solvent tail. Indeed, **5** retained a high level of JAK1 potency (IC_{50} = 0.018 μM) with increased JAK2 selectivity (122-fold). The cyclopropyl amide has also been shown to be a

viable hinge binding motif for JAK1[13] and compound **6** exhibited favorable JAK1 potency (IC_{50} = 0.043 μM) with an encouraging degree of selectivity over JAK2 (60-fold).

We then explored the linkers while keeping the 2-methoxy-1-methyl-aminopyrazole solvent tail group constant. Compound **7,** with a benzylic amine linker, exhibited favorable JAK1 potency (IC_{50} = 0.004 μM), but with low solubility (< 0.1 μM). With the reversed amide linker, compound **8** displayed diminished JAK1 potency (IC_{50} = 0.26 μM). This suggested the amido-linker in **5** is critical for achieving a high level of JAK1 potency. We therefore elected to use this linker for further SAR exploration.

Having leads with promising selectivity between JAK1 and JAK2, we were keen to further evaluate their broader kinase selectivity. To this end, **5** was tested as representative of the chemical series in a panel of 293 kinases at a single point concentration (1 μM). To our disappointment, **5** promiscuously inhibited a broad set of kinases in this panel (80 out of 289 members tested with over 50% inhibitory effect at this concentration. For details, see SI Table 1).

To gain additional structural insights, an X-ray structure of **5**-bound to the JAK1 kinase domain was obtained. Shown in Figure 2 (6SMB), **5** displayed the expected binding mode: the amino pyrimidine moiety forms a two-point binding interaction with the kinase hinge, consistent with our docked pose for compound **3**. Notably, a distinct bidentate hydrogen bond interaction of the indole NH and amide moiety with the carboxylate sidechain of Asp1021 was observed. Gratifyingly, the interaction between the pyridyl group in **5** and imidazole sidechain of His885 was also observed and stabilized the p-loop region, with clear electron density in the

X-ray structure, thus presumably rendering isoform selectivity in a similar manner to that described for **2**. In addition to the p-loop stabilization, the methoxy functionality on the pyrazole solvent tail group, which also potentially contributes to this isoform selectivity, points towards a small hydrophobic pocket defined by the phenyl ring of Phe958 (side chain) and backbone of Pro960, Ser961 and Gly962 in JAK1. The corresponding pocket in JAK2 is formed by the side chain of Tyr931 and the amide backbones of Pro933, Tyr 834 and Gly934. We reasoned that the pocket with a tyrosine residue in JAK2 was more sterically demanding than the one defined by phenylalanine in JAK1. The methoxy-pyrazole solvent tail of **5** is therefore less well tolerated when bound to JAK2 protein, thus leading to diminished activity.

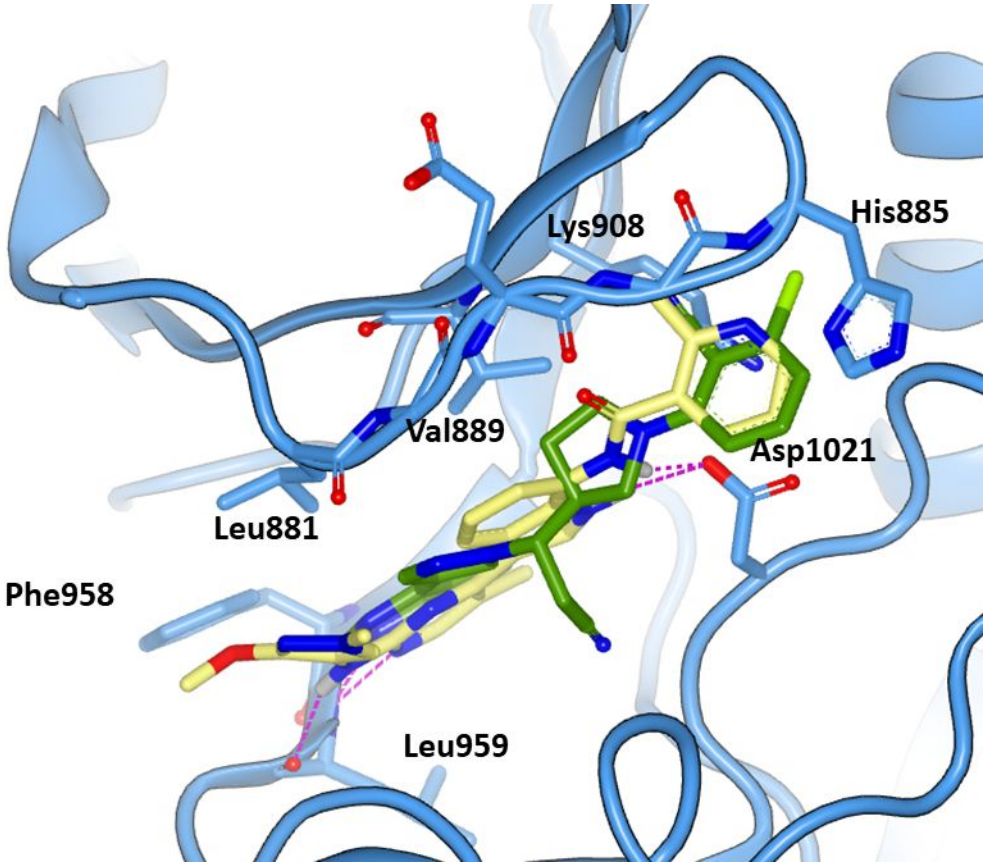

Figure 2. X-ray structure of **5**-JAK1 complex (6SMB). The aminopyrimidine moiety maintains the key hydrogen bonds to the hinge. The amido-indole forms a bidentate hydrogen bond interaction with the side chain carboxylate of Asp1021. The methyl pyridine group forms several hydrophobic interactions in addition to a cation-π interaction with Lys908. Hydrogen bonds are shown as dotted lines. Compound **5** (yellow carbon atoms) overlays with x-ray crystal structure of JAK1 in complex with compound **2** (green carbon atoms).

With this structural information in hand, we set out to improve the broader kinome selectivity of the series, while also attempting to identify leads with better physical properties and improved metabolic stability. In protein kinases, the p-loop regions are flexible with highly diversified structures.[39] We reasoned that a selective kinase inhibitor might be obtained by further exploiting the interaction in this area of the protein. We synthesized over 300 amide analogs of **6**, using a diverse reagent set, comprising aromatic and aliphatic carboxylic acids, while keeping the cyclo-propyl amide solvent tail group constant.[41] All compounds synthesized were tested in our JAK1 and JAK2 biochemical assays, and in parallel their solubility and human microsome clearance (CL_{int}) was measured. Figure 3 shows the JAK1 biochemical potency versus human microsomal CL_{int}, with points colored by the ratio of the IC_{50}s of JAK1 over JAK2, and sized by measured solubility at pH=7.4. While most of compounds in the library displayed low solubility or low JAK2 selectivity, we found that compound **9** (Table 3) had a favorable balance of JAK1 potency and selectivity (JAK1 IC_{50} = 180 nM and more than 166-fold selectivity), with good aqueous solubility (>1000 μM) and low

human microsome CL_{int} (4.4 μL/min/mg). Given the low kinome selectivity of lead compound **5**, we next tested **9** in the kinase panel described previously. Remarkably, **9** displayed an improved kinase selectivity (with only 6 out of 293 kinases tested over 50% inhibition at single dose concentration of 1 μM, see complete kinome screen data in supporting information SI Table 2).

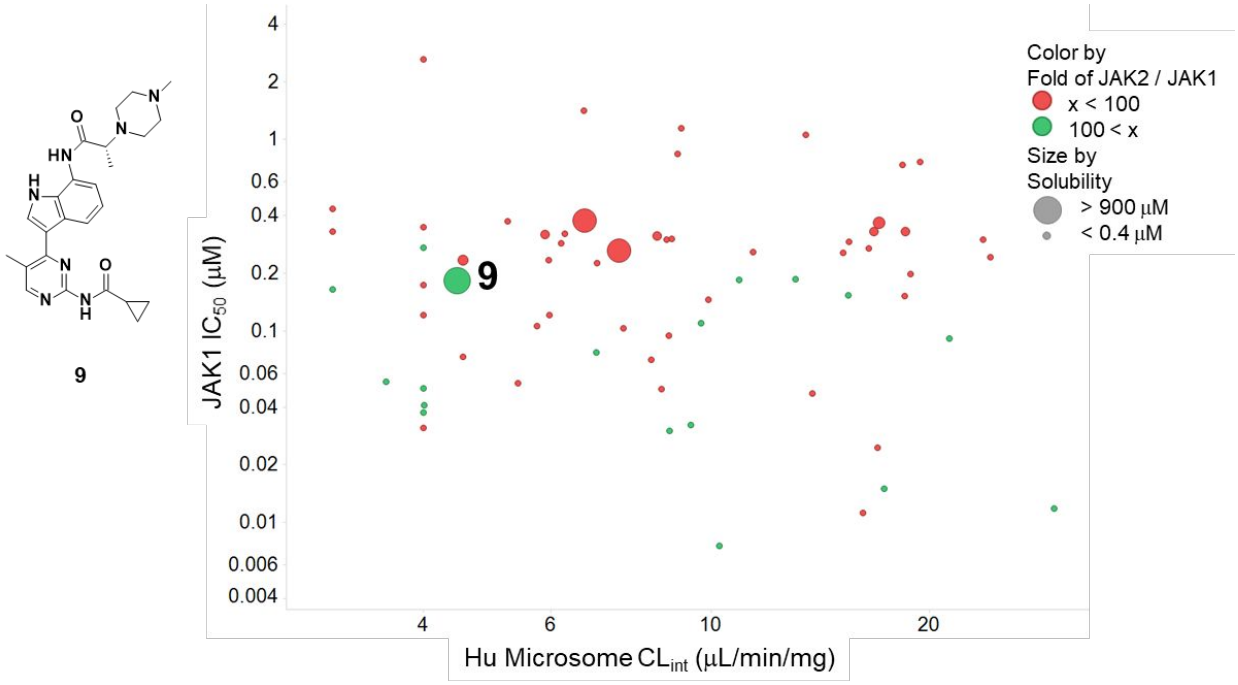

Figure 3. Plot of JAK1 biochemical potency vs. human microsome Cl_{int}. Compound **9** was identified with a favorable balance of potency and properties. Dots were colored by ratio of IC_{50}'s of JAK1 over JAK2 and sized by measured solubility at pH=7.4.

As compound **9** bears a significant structural difference from **5**, an X-ray structure of **9**-bound JAK1 protein was obtained to elucidate its binding mode (Figure 3). The interaction at the hinge and the bidentate interaction of the indole NH and amide NH towards Asp1021 of JAK1 are all maintained. Interestingly, an additional salt-bridge interaction between the chiral piperazine moiety and Asp1003 is also evident in the crystal structure. While the X-ray structure

also shows a stabilized p-loop with clear electron density, the ligand does not form a direct π-π interactions with the loop residues due to lack of an aromatic ring in this region. As Asp1003 is actually conserved between JAK2 and JAK1, we believe it is the combination of the additional polar interaction, p-loop stabilization and the selective nature of the solvent tail group that contributes to the favorable JAK1/2 selectivity of **9**.

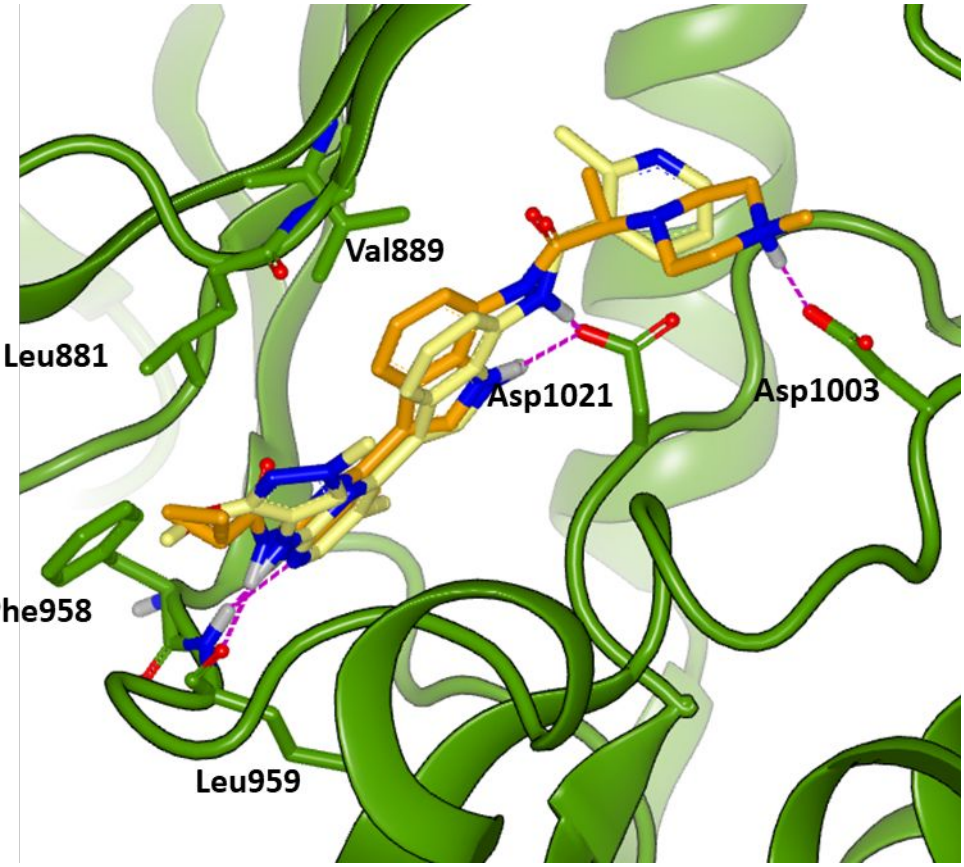

Figure 4. X-ray structure of **9**-JAK1 complex (PDB code: 6GGH). In addition to the retained interactions with the hinge and Aps1021, compound **9** also forms a salt-bridge interaction between the piperazine moiety and Asp1003. Hydrogen bonds are shown as dotted lines. . Compound **9** (orange carbon atoms) overlays with x-ray crystal structure of JAK1 in complex with compound **5** (yellow carbon atoms).

Encouraged by the profile of **9**, we set out to explore the SAR around the chiral basic amides. As shown in Table 3, the *R* configuration in **9** is preferred (JAK1 IC_{50} = 0.18 μM), over its enantiomer **10** (JAK1 IC_{50} = 1.1 μM). Achiral compounds, such as **11** and **12**, exhibited weaker JAK1 activity (IC_{50} = 0.46 μM and 1.7 μM, respectively). As suggested in the crystal structure, the distal basic center of the chiral amide in **9** is essential for JAK1 potency. Removal of the basic centers significantly lowered JAK1 potency (**13**, IC_{50} = 2.4 μM and **14**, IC_{50} = 2.2 μM). Gratifyingly, even though the analogs in Table 3 have various level of JAK1 potency, they consistently displayed high aqueous solubility, indicating the chemical series has favorable physical properties.

Table 3. Structure, JAK enzymatic activity and solubility of compounds **9-14.**

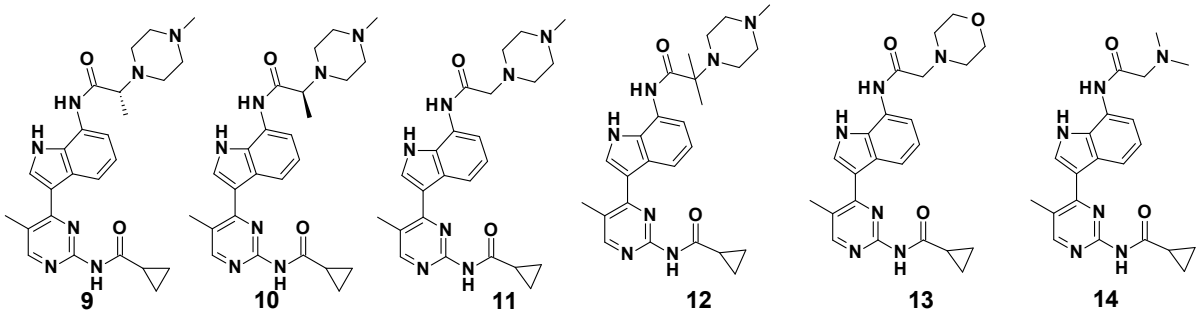

Compound	JAK1 IC_{50} (μM)[a]	JAK2 IC_{50} (μM)[a]	Selectivity over JAK2 (fold)	Solubility (μM)[b]
9	0.18	>30	>166	>930
10	1.1	> 30	>27	>1000
11	0.46	> 30	> 65	230
12	1.7	> 30	>18	>1000
13	2.4	>30	>12	--
14	2.2	>30	> 13	--

[a]Biochemical potency was measured at 5 mM ATP concentration. Selectivity expressed as the ratio of JAK2 IC_{50} over JAK1 IC_{50}. All experimental values represent the geometric mean of at least two independent experiments and have SEM within 0.2 log units. For experimental details, see the supporting information.[22] [b]Solubility measured at pH 7.4.

Establishing that the initial *R*-methyl piperazine was the preferred amine, we set out to explore SAR of the solvent tail groups with this newly identified piperazine amide. Having learned that a small *ortho*-substitution played a critical role in achieving a high level of JAK2 selectivity, we scanned additional *ortho*-substituted aromatic rings. A series of compounds with a high level of JAK1 selectivity were obtained by deploying this tactic (Table 4). Compound **15** with a 2-methylpyridine solvent tail displayed a high degree of JAK1/2 selectivity, albeit at the expense of JAK1 potency (**15**, JAK1 IC_{50} = 0.13 μM). In contrast, installation of a less-sterically demanding *ortho*-substituent, such as F, restored JAK1 potency while maintaining a high JAK1 selectivity (**16**, JAK1 IC_{50} = 0.027 μM, >1000-fold selectivity versus JAK2). As previously described, the *ortho*-methoxy pyrazole solvent tail was well-tolerated (**17**, JAK1 IC_{50} = 0.010 μM, 540-fold selectivity versus JAK2). Having high JAK1 biochemical potency, these compounds were subsequently evaluated in a cellular assay, measuring the inhibition of phosphorylation of STAT3 (pSTAT3), a downstream substrate of JAK1, in an NCI-H1975 cell line. We found that **15** inhibited pSTAT3 with IC_{50} = 0.18 μM. Compound **16** displayed a promising JAK1 cellular potency (IC_{50} = 0.08 μM), however, disappointingly, the compound was found to inhibit the hERG ion channel (IC_{50} = 10 μM). Compound **17** exhibited a potent cellular activity (IC_{50} = 0.13 μM) without any detectable hERG activity (IC_{50} >100 μM).

Table 4. Structure, JAK enzymatic and cellular activity and **15-17**.

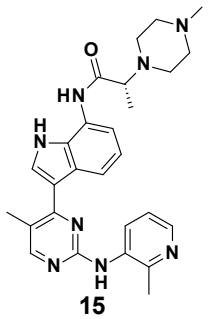

15

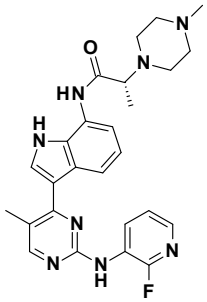

16

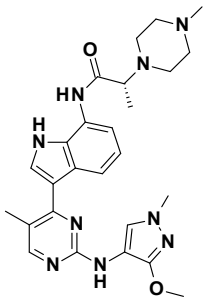

17

Compound	JAK1 IC_{50} (μM)[a]	JAK2 IC_{50} (μM)[a]	Selectivity over JAK2 (folds)	pSTAT3 IC_{50} (μM)[b]	hERG (μM)
15	0.13	> 30	> 230	0.18	> 33
16	0.027	> 30	> 1111	0.08	10
17	0.010	5.4	540	0.13	> 100

[a]Measured at 5 mM ATP concentration. Selectivity expressed as the ratio of JAK2 IC_{50} over JAK1 IC_{50}. All values represent the geometric mean of at least two independent experiments and have SEM within 0.2 log units. [b]Represents cellular mode of action assay measuring inhibition of pSTAT3 in NCI-H1975 cells. For experimental details, see the supporting information.[22]

We next examined the SAR of pyrimidine C5-subsituents. JAK1 possesses a methionine gatekeeper residue, therefore hydrophobic substituents or hydrogen may be favorable at the C-5 position. Shown in the Table 5, increasing hydrophobicity of the substituents led to higher JAK1 potency (**18**, **19**, and **20**, IC_{50} = 7, 19, and 8 nM respectively), however, we also observed the same trend with JAK2 potency. In addition, **18** and **20** exhibited improved cellular potencies (IC_{50} = 0.06 μM and 0.094 μM, respectively), but also displayed moderate hERG ion channel activities (IC_{50} = 22 μM and 15 μM, respectively). Overall, **21**, with a C5-H substituent exhibited the desired balance of favorable JAK1 potency, selectivity versus JAK2, and no detectable hERG activity. We therefore selected it for further profiling.

Table 5. Structure, JAK enzymatic and cellular activity of **18-21**

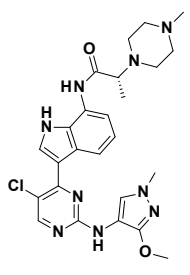

18

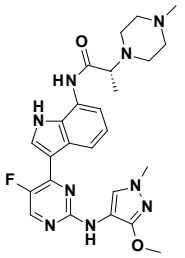

19

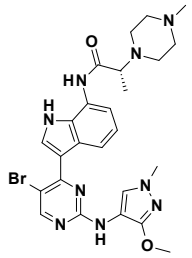

20

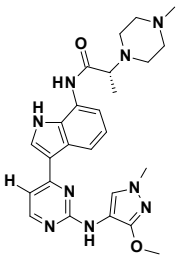

21

Compound	JAK1 IC_{50} (μM)[a]	JAK2 IC_{50} (μM)[a]	Selectivity over JAK2 (folds)	pSTAT3 IC_{50} (μM)[b]	hERG (μM)
18	0.007	1.80	257	0.060	22
19	0.019	6.60	347	0.12	> 33
20	0.008	1.57	196	0.094	15
21	0.070	>15	>214	0.130	> 100

[a]Measured at 5 mM ATP concentration. Selectivity expressed as the ratio of JAK2 IC_{50} over JAK1 IC_{50}. All values represent the geometric mean of at least two independent experiments and have SEM within 0.2 log units. [b]Represents cellular mode of action assay measuring inhibition of pSTAT3 in NCI-H1975 cells. For experimental details, see the supporting information.[22]

Having **21** with high selectivity between JAK1 and JAK2, first we tested **21** in the biochemical assays of other JAK family kinases with a high concentration of ATP and found that **21** is inactive toward JAK3 (IC_{50} > 30 μM) with only moderate activity toward TYK2 (IC_{50} = 2.8 μM). Next, in a panel of 293 kinases at single point concentration (1 μM), we found that **21** showed a high level of selectivity, only inhibiting one other kinase (FLT4) over 75% at this concentration (for details, see supporting information SI Table 3).

Compound **21** displayed high metabolic stability in hepatocyte CL_{int} assays across species, with high solubility at pH=6.5 (> 1000 μM) (Table 6). Compound **21** did not inhibit any of the isoforms of human cytochrome P450s up to a concentration of 30 μM. Compound **21** also displayed high permeability (Papp = 7.5 $1x10^{-6}$ cm/s) with a low efflux ratio (2.6) in a Caco-2 assay (Table 6). Compound **21** displayed favorable pharmacokinetic properties across

species (Table 7), showing a low *in vivo* clearance (20 mL/min/kg) with a moderate half-life (6 hours) and excellent oral bioavailability (100%) in rats. We similarly observed that **21** has low *in vivo* clearance (9 mL/min/kg) with prolonged half-life (9 hour) and high oral availability (71%) in dogs.

Table 6. Preclinical ADME and calculated properties of **21**

Log D at pH7.4[a]	Solubility at pH 6.5 (μM)[b]	Hepatocyte[c] Cl_{int} ((μL/min)/10^{-6} cells) Rat, dog, human	Human cytochrome P450 inhibition IC_{50} (μM) All isoforms	Permeability Caco-2 A to B Papp (1 x 10^{-6} cm/s) (efflux ratio)[d]	Calculated properties		
					M.W	PSA	LogP
1.7	605	<1.9, 2.0, <1	> 30	7.5 (2.6)	489	106	1.4

[a]Measured using shake-flask methodology with a buffer:octanol volume ratio of 100:1. at pH 7.4. [b] High-throughput solubility using DMSO stock solution was measured in pH 7.4 phosphate buffer at 37 °C. [c]Intrinsic clearance measured from fresh hepatocytes from the indicated species. [d] Permeability was measured in both the apical to basolateral (A to B) and basolateral to apical (B to A) direction. Efflux ratio (ER) determined as the ratio of both permeabilities (B to A permeability divided by A to B permeability)

Table 7. Pharmacokinetic properties of **21** in rats and dogs

Preclinical species	Route	F%	AUC (μM.hr)	CL(obs) (mL/min/kg)	Vdss (L/kg)	T1/2 (hr)
Rat[a]	i.v.		1.2	20	8.7	6
	p.o.	100%	1.7			7
Dog[b]	i.v.		3.1	9.0	6.3	9
	p.o.	71%	5.3			9

[a] Han Wistar rat male; 10 mg/kg p.o. (0.1% HPMC); 5 mg/kg i.v. (40%DMA/40%PEG/20% saline). [b] Beagle dog male; 20 mg/kg p.o. (0.1% HPMC, pH 2); 10 mg/kg i.v. (20% TEG/D5W).

With advanced compound **21** in hand, we were keen to evaluate its preclinical *in vivo* antitumor activity, and furthermore, to test the hypothesis that inhibition of JAK1 could be a viable therapeutic approach to enhance antitumor activity in combination with the approved therapies targeting oncogenic signaling pathways. In order to see the additive effect, we evaluated **21** (dosed at 50 mpk BID) in a mouse non-small cell lung cancer (NSCLC) xenograft

NCI-H1975 model in combination with the approved third generation mutant EGFR selective kinase inhibitor, osimertinib, **22** at a low dose of 2.5 mpk..[42-43] NCI-H1975 cells were implanted subcutaneously in female NCr nude mice (Taconic Laboratories). Ten days after cell implantation, mice were randomized into groups of 6 to 8 mice (average tumor volume 189 mm^3, range 152 to 250 mm^3), and were dosed orally with either vehicle (20% captisol), **21**, **22**, or combinations of **21** plus **22**, at the doses and schedules indicated in Figure 4 for 18 days. In the combination treated groups, the addition of **21** enhanced the antitumor activity of **22** (green diamonds), compared to treatment with **22** alone (red squares). When compound **21** was administered as a single agent (blue triangles), it had only weak antitumor activity relative to vehicle control treatment (black circles). On the last day of treatment, the inhibition of tumor growth of the combination treatments was statistically significant ($p < 0.05$), compared to single agent **22** alone. All treatments were well tolerated, with no significant weight loss or other outward signs observed over the course of treatment (data not shown).

A satellite group of the tumor bearing mice were treated for a single day with these compounds for pharmacodynamic analysis. We measured pSTAT3 (Y705) levels in tumor lysates as an *in vivo* biomarker of JAK1 kinase inhibition as described previously[22] and pEGFR (Y1173) levels as the biomarker of EGFR (T790M) inhibition.[42-43] A single 2.5 mg/kg dose of **22** achieved a complete inhibition of pEGFR levels up to 24 h. With a 50 mg/kg dose of **21**, approximately 80% of the pSTAT3 inhibition was maintained up to 8 hours after dosing (Figure 5). The combined doses of **21** and **22** resulted in a robust knockdown of pSTAT3 and pEGFR, measured at 8 hours after the dose. This correlated well with the observed enhanced antitumor activity in the mice xenograft efficacy study. Taken together, the increased antitumor activity of **21** plus **22** in combination compared to single agent **22**, and the correlation with pSTAT3

knockdown by **21**, is consistent with a role for STAT3 signaling in escape from, or resistance to, EGFR inhibition in this model. The results support the hypothesis that inhibition of STAT3 signaling can enhance the antitumor activity of an EGFR inhibitor in T790M EGFR mutant NSCLC. As such, compound **21** displayed the best overall profile, and was thus selected as the drug candidate to progress into the clinical development.

Figure 4. Compound **21** enhances the antitumor activity of low dose **22** (osimertinib) in an NCI-H1975 (T790M) NSCLC xenograft model.

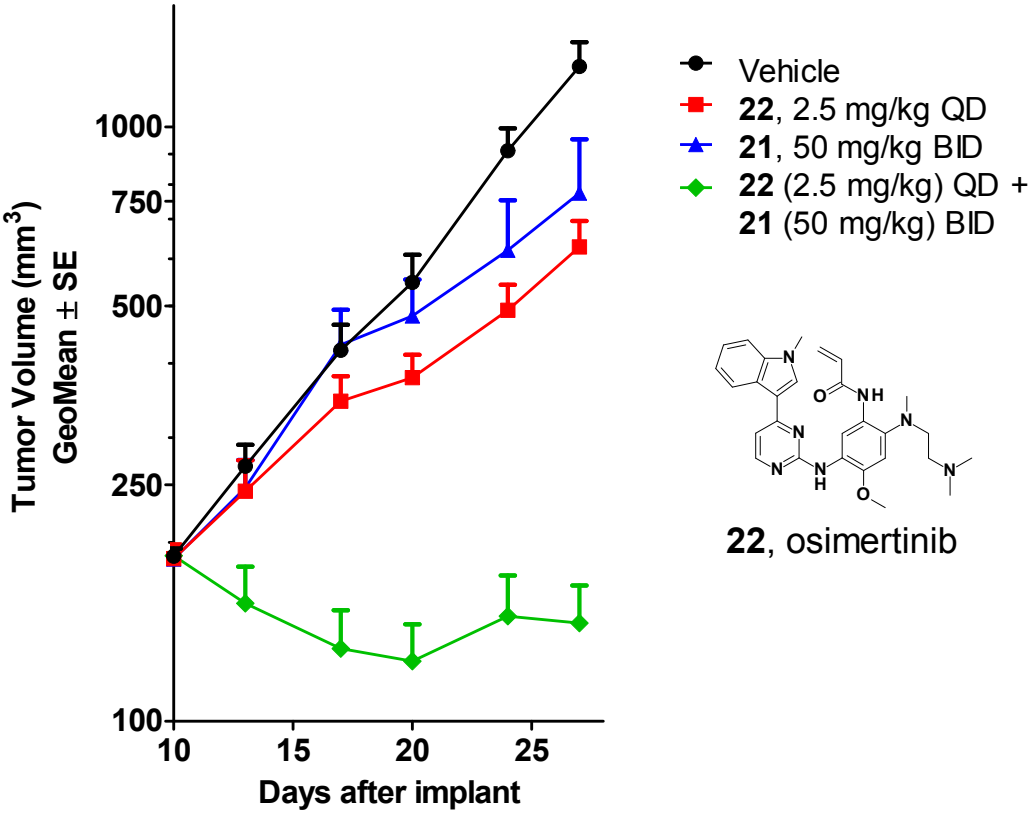

Figure 5. Plot of pSTAT3 and pEGFR signals in an NCI-H1975 mouse xenograft model with the treatment of **21** and **22.**

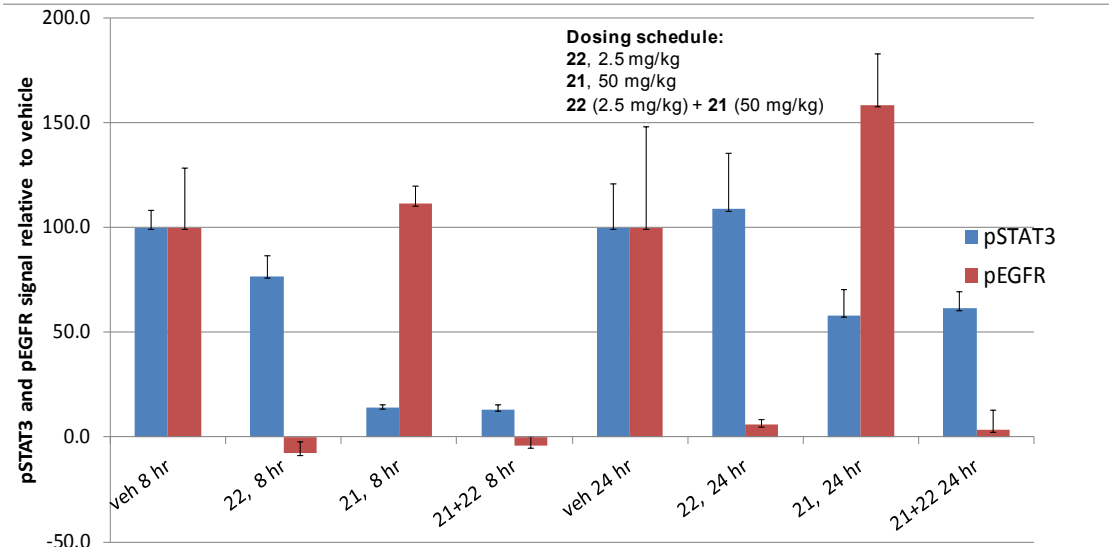

Conclusion

we have described our efforts toward the development of a JAK1 selective inhibitor. Starting from a non-kinome selective screening hit **3**, structure based-design and a parallel synthesis approach were used to identify the potent and selective lead **9**. Further optimization led to the discovery of candidate drug **21** (AZD4205) with a high degree of JAK1 potency and favorable DMPK properties. The compound displayed an enhanced antitumor activity in combination with approved EGFR inhibitor, osimertinib, in a preclinical NSCLC model. These findings warrant the further investigation of **21** in human clinical trials.

Chemistry

Suzuki reactions were used to couple the 7-nitro-indole boronic ester (**SI3**) to 2,4-dichloropyrimidines, differentially substituted at the C-5 position, to furnish 2-chloro-4-indole pyrimidines, i.e ***SI5***. Subsequently an acid-mediated aniline displacement yielded the desired nitro-intermediates. Reduction of the nitro group under mild conditions was followed by amidation to produce the desired compounds (for an example, the synthesis of **21** is described in Scheme 1. For the synthesis of other compounds, see supporting information).

Scheme 1. Example synthesis of compound **21**[a]

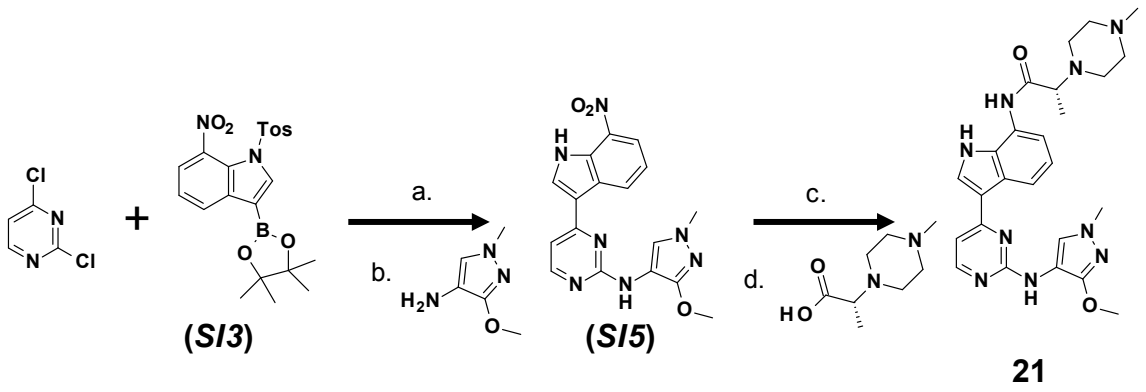

[a]Reagents and conditions: (a) (i) $Pd(dppf)_2$, K_2CO_3; 83 %; (ii) NaOH, 50 °C, 81%; (b) $TsOH.H_2O$, 130 °C, 75%; (c) Fe, NH_4Cl, 74%; (d) HATU, $iPrEt_2N$, 48%.

EXPERIMENTAL

General information

All solvents used were commercially available in anhydrous grade. Reagents were utilized without further purification unless otherwise stated. Evaporation of solvent was carried out using a rotary evaporator under reduced pressure at a bath temperature of up to 60 ºC. Temperatures

are given in degrees Celsius (ºC), and operations were carried out at room or ambient temperature, that is, at a temperature in the range of 18-30 ºC. In general, the course of reactions was followed by thin layer chromatography or mass spectroscopy and reaction times are given for illustration only; where a synthesis is described as being analogous to that described in a previous example, the amounts used are the millimolar ratio equivalents to those used in the previous example. NMR data is in the form of delta values for major diagnostic protons, given in parts per million (ppm) relative to tetramethylsilane (TMS) as an internal standard, determined at 300 MHz or 400 MHz using deuterated solvent. Analytical mass spectra were run with an electron energy of 70 eV in the chemical ionization (CI) mode using a direct exposure probe; where indicated ionization was effected by electron impact (EI), electrospray (ESP), or atmospheric pressure chemical ionization (APCI); values for m/z are given; generally, only ions which indicate the parent mass are reported. Unless otherwise indicated, all final compounds were purified to ≥95% purity, as assessed by analytical HPLC using an Agilent 1100 equipped with Waters columns (Atlantis T3, 2.1 × 50 mm, 3 μm or Atlantis C18, 2.1 × 50 mm, 5 μm) eluted for >10 min with a gradient mixture of water and acetonitrile with either formic acid or ammonium acetate added as a modifier, monitored at wavelengths of 220, 254, and 280 nm.

All experimental activities involving animals were carried out in accordance with AstraZeneca animal welfare protocols, which are consistent with The American Chemical Society Publications rules and ethical guidelines. For details of synthesis, please see supporting information.

ASSOCIATED CONTENT

Supporting information is available free of charge via the Internet at http://pubs.acs.org including compound synthesis, characterization, crystallographic information, and kinase panel selectivity data, additional DMPK data, compound purity data, NMR spectra of selected compounds and molecular formula strings of the compounds.

Author information:

Corresponding Author:

*Tel.: + +1 781-839-4175. E-mail: qibin.su@astrazeneca.com.

Author Contributions:

The manuscript was written through contributions of all authors. All authors have given approval to the final version of the manuscript.

Acknowledgement:

Authors would like to thank Dr Brian Aquila for insightful discussion, Dr. Michelle Lamb for proofreading the manuscript, Dr. Kun Song for preparing structure pictures, Sharon Tentarelli for LC/MS support and Holger Steuber for obtaining the x-ray crystal structures.

Notes:

The authors declare no competing financial interest.

Abbreviations:

Jak2, Janus kinase 2; Jak1, Janus kinase 1; Jak3, Janus kinase 3; MF, idiopathic myelofibrosis; mpk, mg/kg; MPNs, myeloproliferative neoplasms; PAGE, Polyacrylamide gel electrophoresis; PEG, polyethylene glycol; PV, polycythemia vera; SDS, sodium dodecyl sulfate; STAT, signal transducers and activators of transcription; pSTAT, phosphorylated signal transducers and activators of transcription; tSTAT, total signal transducers and activators of transcription; TGI, tumor growth inhibition; Tyk2, tyrosine kinase 2.

Reference:

1. Hammaren, H. M.; Virtanen, A. T.; Raivola, J.; Silvennoinen, O., The regulation of JAKs in cytokine signaling and its breakdown in disease. *Cytokine* **2019,** *118*, 48-63.

2. Vakil, E.; Tefferi, A., BCR-ABL1--negative myeloproliferative neoplasms: a review of molecular biology, diagnosis, and treatment. *Clin Lymphoma Myeloma Leuk* **2011,** *11 Suppl 1*, S37-45.

3. Kiu, H.; Nicholson, S. E., Biology and significance of the JAK/STAT signalling pathways. *Growth Factors* **2012,** *30* (2), 88-106.

4. Flanagan, M. E.; Blumenkopf, T. A.; Brissette, W. H.; Brown, M. F.; Casavant, J. M.; Shang-Poa, C.; Doty, J. L.; Elliott, E. A.; Fisher, M. B.; Hines, M.; Kent, C.; Kudlacz, E. M.; Lillie, B. M.; Magnuson, K. S.; McCurdy, S. P.; Munchhof, M. J.; Perry, B. D.; Sawyer, P. S.; Strelevitz, T. J.; Subramanyam, C.; Sun, J.; Whipple, D. A.; Changelian, P. S., Discovery of CP-690,550: a potent and selective Janus kinase (JAK) inhibitor for the treatment of autoimmune diseases and organ transplant rejection. *J Med Chem* **2010,** *53* (24), 8468-8484.

5. Verstovsek, S.; Kantarjian, H.; Mesa, R. A.; Pardanani, A. D.; Cortes-Franco, J.; Thomas, D. A.; Estrov, Z.; Fridman, J. S.; Bradley, E. C.; Erickson-Viitanen, S.; Vaddi, K.; Levy, R.; Tefferi, A., Safety and efficacy of INCB018424, a JAK1 and JAK2 inhibitor, in myelofibrosis. *N Engl J Med* **2010,** *363* (12), 1117-1127.

6. Papp, K. A.; Menter, M. A.; Raman, M.; Disch, D.; Schlichting, D. E.; Gaich, C.; Macias, W.; Zhang, X.; Janes, J. M., A randomized phase 2b trial of baricitinib, an oral Janus kinase (JAK) 1/JAK2 inhibitor, in patients with moderate-to-severe psoriasis. *Br J Dermatol* **2016,** *174* (6), 1266-1276.

7. Genovese, M. C.; Kremer, J.; Zamani, O.; Ludivico, C.; Krogulec, M.; Xie, L.; Beattie, S. D.; Koch, A. E.; Cardillo, T. E.; Rooney, T. P.; Macias, W. L.; de Bono, S.; Schlichting, D. E.; Smolen, J. S., Baricitinib in patients with refractory rheumatoid arthritis. *N Engl J Med* **2016,** *374* (13), 1243-1252.

8. Genovese, M. C.; Greenwald, M.; Codding, C.; Zubrzycka-Sienkiewicz, A.; Kivitz, A. J.; Wang, A.; Shay, K.; Wang, X.; Garg, J. P.; Cardiel, M. H., Peficitinib, a JAK inhibitor, in combination with limited conventional synthetic disease-modifying antirheumatic drugs in the treatment of moderate-to-severe rheumatoid arthritis. *Arthritis Rheumatol* **2017,** *69* (5), 932-942.

9. Kivitz, A. J.; Gutierrez-Urena, S. R.; Poiley, J.; Genovese, M. C.; Kristy, R.; Shay, K.; Wang, X.; Garg, J. P.; Zubrzycka-Sienkiewicz, A., Peficitinib, a JAK inhibitor, in the treatment of moderate-to-severe rheumatoid arthritis in patients with an inadequate response to methotrexate. *Arthritis Rheumatol* **2017,** *69* (4), 709-719.

10. Kettle, J. G.; Astrand, A.; Catley, M.; Grimster, N. P.; Nilsson, M.; Su, Q.; Woessner, R., Inhibitors of JAK-family kinases: an update on the patent literature 2013-2015, part 1. *Expert Opin Ther Pat* **2017,** *27* (2), 127-143.

11. Genovese, M. C.; Smolen, J. S.; Weinblatt, M. E.; Burmester, G. R.; Meerwein, S.; Camp, H. S.; Wang, L.; Othman, A. A.; Khan, N.; Pangan, A. L.; Jungerwirth, S., Efficacy and safety of ABT-494, a selective JAK-1 inhibitor, in a phase IIb study in patients with rheumatoid arthritis and an inadequate response to methotrexate. *Arthritis Rheumatol* **2016,** *68* (12), 2857-2866.

12. Vazquez, M. L.; Kaila, N.; Strohbach, J. W.; Trzupek, J. D.; Brown, M. F.; Flanagan, M. E.; Mitton-Fry, M. J.; Johnson, T. A.; TenBrink, R. E.; Arnold, E. P.; Basak, A.; Heasley, S. E.; Kwon, S.; Langille, J.; Parikh, M. D.; Griffin, S. H.; Casavant, J. M.; Duclos, B. A.; Fenwick, A. E.; Harris, T. M.; Han, S.; Caspers, N.; Dowty, M. E.; Yang, X.; Banker, M. E.; Hegen, M.; Symanowicz, P. T.; Li, L.; Wang, L.; Lin, T. H.; Jussif, J.; Clark, J. D.; Telliez, J. B.; Robinson, R. P.; Unwalla, R., Identification of N-{cis-3-[Methyl(7H-pyrrolo[2,3-d]pyrimidin-4-yl)amino]cyclobutyl}propane-1-sulfonamide (PF-04965842): a selective JAK1 clinical candidate for the treatment of autoimmune diseases. *J Med Chem* **2018,** *61* (3), 1130-1152.

13. Van Rompaey, L.; Galien, R.; van der Aar, E. M.; Clement-Lacroix, P.; Nelles, L.; Smets, B.; Lepescheux, L.; Christophe, T.; Conrath, K.; Vandeghinste, N.; Vayssiere, B.; De Vos, S.; Fletcher, S.; Brys, R.; van 't Klooster, G.; Feyen, J. H.; Menet, C., Preclinical characterization of GLPG0634, a selective inhibitor of JAK1, for the treatment of inflammatory diseases. *J Immunol* **2013,** *191* (7), 3568-3577.

14. Menet, C. J.; Mammoliti, O.; Lopez-Ramos, M., Progress toward JAK1-selective inhibitors. *Future Med Chem* **2015,** *7* (2), 203-235.

15. Menet, C. J.; Rompaey, L. V.; Geney, R., Advances in the discovery of selective JAK inhibitors. *Prog Med Chem* **2013,** *52*, 153-223.

16. Ioannidis, S.; Lamb, M. L.; Davies, A. M.; Almeida, L.; Su, M.; Bebernitz, G.; Ye, M.; Bell, K.; Alimzhanov, M.; Zinda, M., Discovery of pyrazol-3-ylamino pyrazines as novel JAK2 inhibitors. *Bioorg Med Chem Lett* **2009,** *19* (23), 6524-6538.

17. Ioannidis, S.; Lamb, M. L.; Almeida, L.; Guan, H.; Peng, B.; Bebernitz, G.; Bell, K.; Alimzhanov, M.; Zinda, M., Replacement of pyrazol-3-yl amine hinge binder with thiazol-2-yl amine: Discovery of potent and selective JAK2 inhibitors. *Bioorg Med Chem Lett* **2010,** *20* (5), 1669-1673.

18. Wang, T.; Ioannidis, S.; Almeida, L.; Block, M. H.; Davies, A. M.; Lamb, M. L.; Scott, D. A.; Su, M.; Zhang, H. J.; Alimzhanov, M.; Bebernitz, G.; Bell, K.; Zinda, M., In vitro and in vivo evaluation of 6-aminopyrazolyl-pyridine-3-carbonitriles as JAK2 kinase inhibitors. *Bioorg Med Chem Lett* **2011,** *21* (10), 2958-2961.

19. Guan, H.; Lamb, M. L.; Peng, B.; Huang, S.; Degrace, N.; Read, J.; Hussain, S.; Wu, J.; Rivard, C.; Alimzhanov, M.; Bebernitz, G.; Bell, K.; Ye, M.; Zinda, M.; Ioannidis, S., Discovery of novel Jak2-Stat pathway inhibitors with extended residence time on target. *Bioorg Med Chem Lett* **2013,** *23* (10), 3105-3110.

20. Su, Q.; Ioannidis, S.; Chuaqui, C.; Almeida, L.; Alimzhanov, M.; Bebernitz, G.; Bell, K.; Block, M.; Howard, T.; Huang, S.; Huszar, D.; Read, J. A.; Rivard Costa, C.; Shi, J.; Su, M.; Ye, M.; Zinda, M., Discovery of 1-methyl-1H-imidazole derivatives as potent Jak2 inhibitors. *J Med Chem* **2014,** *57* (1), 144-158.

21. Vasbinder, M. M.; Alimzhanov, M.; Augustin, M.; Bebernitz, G.; Bell, K.; Chuaqui, C.; Deegan, T.; Ferguson, A. D.; Goodwin, K.; Huszar, D.; Kawatkar, A.; Kawatkar, S.; Read, J.; Shi, J.; Steinbacher, S.; Steuber, H.; Su, Q.; Toader, D.; Wang, H.; Woessner, R.; Wu, A.; Ye, M.; Zinda, M., Identification of azabenzimidazoles as potent JAK1 selective inhibitors. *Bioorg Med Chem Lett* **2016,** *26* (1), 60-67.

22. Grimster, N. P.; Anderson, E.; Alimzhanov, M.; Bebernitz, G.; Bell, K.; Chuaqui, C.; Deegan, T.; Ferguson, A. D.; Gero, T.; Harsch, A.; Huszar, D.; Kawatkar, A.; Kettle, J. G.; Lyne, P.; Read, J. A.; Rivard Costa, C.; Ruston, L.; Schroeder, P.; Shi, J.; Su,

Q.; Throner, S.; Toader, D.; Vasbinder, M.; Woessner, R.; Wang, H.; Wu, A.; Ye, M.; Zheng, W.; Zinda, M., Discovery and optimization of a novel series of highly selective JAK1 kinase inhibitors. *J Med Chem* **2018,** *61* (12), 5235-5244.

23. Turkson, J.; Jove, R., STAT proteins: novel molecular targets for cancer drug discovery. *Oncogene* **2000,** *19* (56), 6613-6626.

24. Zamo, A.; Chiarle, R.; Piva, R.; Howes, J.; Fan, Y.; Chilosi, M.; Levy, D. E.; Inghirami, G., Anaplastic lymphoma kinase (ALK) activates Stat3 and protects hematopoietic cells from cell death. *Oncogene* **2002,** *21* (7), 1038-1047.

25. Sansone, P.; Bromberg, J., Targeting the interleukin-6/Jak/stat pathway in human malignancies. *J Clin Oncol* **2012,** *30* (9), 1005-1014.

26. Niu, G.; Bowman, T.; Huang, M.; Shivers, S.; Reintgen, D.; Daud, A.; Chang, A.; Kraker, A.; Jove, R.; Yu, H., Roles of activated Src and Stat3 signaling in melanoma tumor cell growth. *Oncogene* **2002,** *21* (46), 7001-7010.

27. Kortylewski, M.; Jove, R.; Yu, H., Targeting STAT3 affects melanoma on multiple fronts. *Cancer Metastasis Rev* **2005,** *24* (2), 315-327.

28. Huang, M.; Page, C.; Reynolds, R. K.; Lin, J., Constitutive activation of stat 3 oncogene product in human ovarian carcinoma cells. *Gynecol Oncol* **2000,** *79* (1), 67-73.

29. Horiguchi, A.; Oya, M.; Shimada, T.; Uchida, A.; Marumo, K.; Murai, M., Activation of signal transducer and activator of transcription 3 in renal cell carcinoma: a study of incidence and its association with pathological features and clinical outcome. *J Urol* **2002,** *168* (2), 762-765.

30. Corvinus, F. M.; Orth, C.; Moriggl, R.; Tsareva, S. A.; Wagner, S.; Pfitzner, E. B.; Baus, D.; Kaufmann, R.; Huber, L. A.; Zatloukal, K.; Beug, H.; Ohlschlager, P.; Schutz, A.; Halbhuber, K. J.; Friedrich, K., Persistent STAT3 activation in colon cancer is associated with enhanced cell proliferation and tumor growth. *Neoplasia* **2005,** *7* (6), 545-555.

31. Chang, K. C.; Wu, M. H.; Jones, D.; Chen, F. F.; Tseng, Y. L., Activation of STAT3 in thymic epithelial tumours correlates with tumour type and clinical behaviour. *J Pathol* **2006,** *210* (2), 224-33.

32. Yin, Z.; Zhang, Y.; Li, Y.; Lv, T.; Liu, J.; Wang, X., Prognostic significance of STAT3 expression and its correlation with chemoresistance of non-small cell lung cancer cells. *Acta Histochem* **2012,** *114* (2), 151-158.

33. Thomas, S. J.; Snowden, J. A.; Zeidler, M. P.; Danson, S. J., The role of JAK/STAT signalling in the pathogenesis, prognosis and treatment of solid tumours. *Br J Cancer* **2015,** *113* (3), 365-371.

34. Gao, S. P.; Mark, K. G.; Leslie, K.; Pao, W.; Motoi, N.; Gerald, W. L.; Travis, W. D.; Bornmann, W.; Veach, D.; Clarkson, B.; Bromberg, J. F., Mutations in the EGFR kinase domain mediate STAT3 activation via IL-6 production in human lung adenocarcinomas. *J Clin Invest* **2007,** *117* (12), 3846-3856.

35. Sun, L.; Ma, K.; Wang, H.; Xiao, F.; Gao, Y.; Zhang, W.; Wang, K.; Gao, X.; Ip, N.; Wu, Z., JAK1-STAT1-STAT3, a key pathway promoting proliferation and preventing premature differentiation of myoblasts. *J Cell Biol* **2007,** *179* (1), 129-138.

36. O'Shea, J. J.; Holland, S. M.; Staudt, L. M., JAKs and STATs in immunity, immunodeficiency, and cancer. *N Engl J Med* **2013,** *368* (2), 161-170.

37. Kettle, J. G.; Astrand, A.; Catley, M.; Grimster, N. P.; Nilsson, M.; Su, Q.; Woessner, R., Inhibitors of JAK-family kinases: an update on the patent literature 2013-2015, part 2. *Expert Opin Ther Pat* **2017,** *27* (2), 145-161.

38. Rodgers, J. D. S., S.; Arvanitis, A. G.; Wang, H.; Storace, L.; Folmer, B.; Shao, L.; Zhu, W.; Glenn, J. P., Preparation of N-(hetero)arylpyrrolidine Derivatives of Pyrazol-4-ylpyrrolo[2,3-d]pyrimidines and Pyrrol-3-ylpyrrolo[2,3-d]pyrimidines as Janus Kinase JAK1 Inhibitors. *PCT Int. Appl.* **2010**, WO 2010135650 A120101125.

39. Nolen, B.; Taylor, S.; Ghosh, G., Regulation of protein kinases; controlling activity through activation segment conformation. *Mol Cell* **2004,** *15* (5), 661-675.

40. Lyne, P. D.; Lamb, M. L.; Saeh, J. C., Accurate prediction of the relative potencies of members of a series of kinase inhibitors using molecular docking and MM-GBSA scoring. *J Med Chem* **2006,** *49* (16), 4805-4808.

41. Aastrand, A. B., Grimster, N. P.; Kawatkar, S.; Kettle, J. G.; Nilsson, M. K..; Ruston, L. L.; Su, Q.; Vasbinder, M. M.; Winter-Holt, J. J.; Wu, D.; Yang, W.; Grecu, T.; McCabe, J.; Woessner, R. D.; Chuaqui, C. E. , Preparation of Substituted 2-(piperazin-1-yl)-N-[3-[2-[(1H-pyrazol-4-yl)amino]pyrimidin-4-yl]-1H-indol-7-yl]

Propanamide as Selective JAK1 Inhibitors for Treating Cancers and Immune Disorders. *PCT Int. Appl.* **2017**, WO201750938.

42. Ward, R. A.; Anderton, M. J.; Ashton, S.; Bethel, P. A.; Box, M.; Butterworth, S.; Colclough, N.; Chorley, C. G.; Chuaqui, C.; Cross, D. A.; Dakin, L. A.; Debreczeni, J. E.; Eberlein, C.; Finlay, M. R.; Hill, G. B.; Grist, M.; Klinowska, T. C.; Lane, C.; Martin, S.; Orme, J. P.; Smith, P.; Wang, F.; Waring, M. J., Structure- and reactivity-based development of covalent inhibitors of the activating and gatekeeper mutant forms of the epidermal growth factor receptor (EGFR). *J Med Chem* **2013,** *56* (17), 7025-7048.

43. Finlay, M. R.; Anderton, M.; Ashton, S.; Ballard, P.; Bethel, P. A.; Box, M. R.; Bradbury, R. H.; Brown, S. J.; Butterworth, S.; Campbell, A.; Chorley, C.; Colclough, N.; Cross, D. A.; Currie, G. S.; Grist, M.; Hassall, L.; Hill, G. B.; James, D.; James, M.; Kemmitt, P.; Klinowska, T.; Lamont, G.; Lamont, S. G.; Martin, N.; McFarland, H. L.; Mellor, M. J.; Orme, J. P.; Perkins, D.; Perkins, P.; Richmond, G.; Smith, P.; Ward, R. A.; Waring, M. J.; Whittaker, D.; Wells, S.; Wrigley, G. L., Discovery of a potent and selective EGFR inhibitor (AZD9291) of both sensitizing and T790M resistance mutations that spares the wild type form of the receptor. *J Med Chem* **2014,** *57* (20), 8249-8267.

TOC

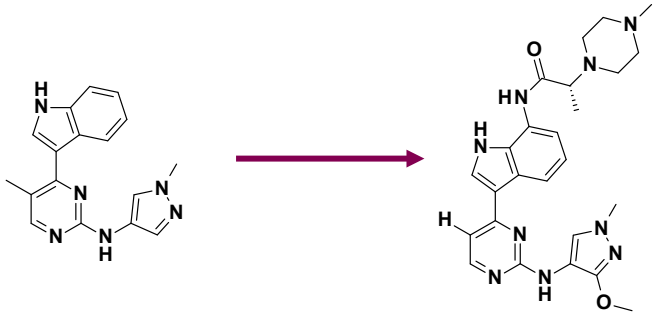

3

JAK1 IC_{50} = 0.07 μM
JAK2 IC_{50} = 0.38 μM

21 (AZD4205)

JAK1 IC_{50} = 0.07 μM
JAK2 IC_{50} > 15 μM